Structural, magnetic and magnetotransport properties of $Pr_{1-x}Sr_xMnO_3$ (x=0.2, 0.3 &0.5) synthesized by co-precipitation method

U. CHAND, K. YADAV, A. GAUR[a*], G. D. VARMA
Department of Physics, Indian Institute of Technology, Roorkee-247667, India
[a]*Department of Physics, National Institute of Technology, Kurukshetra-136116, India*

In this work, we synthesized the $Pr_{1-x}Sr_xMnO_3$ (x = 0.2, 0.3 and 0.5) samples via improved chemical co-precipitation method and studied their structural, magnetic and magnetotransport properties. XRD results show that the unit cell parameters & cell volume decrease as we increase the Sr concentration from x=0.2 to x=0.5. Temperature dependence magnetization measurements indicate that all sample show the paramagnetic to ferromagnetic transition and the Curie temperature increases from 130 to 292 K for the sample x=0.2 to x=0.5. Moreover, the maximum value of magnetization has been observed for the composition with x=0.3. Temperature dependence electrical resistivity measurements show the metal to insulator transition at 102 and 143 K, respectively for sample x = 0.2 & 0.3. However, sample x= 0.5 shows the insulating behavior in the whole measured temperature range (80-300 K). Furthermore, the magnetoresistance studies show that the maximum (MR) is observed for the composition, x=0.3.

(Received September 8, 2010; accepted November 10, 2010)

Keywords: Magnetoresistance, Electrical transport, Magnetism, Pr-Sr-Mn-O, Co-precipitation method, Pr-Sr-Mn-O, Co-precipitation method

1. Introduction

Colossal magnetoresistive (CMR) materials which have a general formula of $R_{1-x}A_xMnO_3$ where R is a rare earth ion like La, Pr etc and A is an alkaline earth ion like Sr, Ca etc., show a huge change in resistance on application of a magnetic field (~ 99% in a field of about 6-7 T) [1-5]. The transport and magnetic properties in these systems to a first order has been based on the double exchange (DE) mechanism [6]. However, theoretical considerations [7] indicate that the DE mechanism alone could not quantitatively account for large changes in the resistivity and magnetoresistance and a strong electron–phonon coupling which exists in the parent $REMnO_3$ has to be taken into consideration [7, 8]. This coupling exists because of the Jahn-Teller nature of the Mn^{3+} ion which results in spontaneous lattice distortion of the MnO_6 octahedra. Manganites have a rich and diverse phase diagram wherein for low (x<0.2) or high (x>0.5) doping values of the alkaline earth concentration. They behave like ferromagnetic/antiferromagnetic insulators and for an optimal doping of 0.2≤ x ≤0.4 undergo a paramagnetic (PM) to ferromagnetic (FM) transition accompanied by an insulator (I) to metal (M) transition and colossal magnetoresistance. The paramagnetic to ferromagnetic and the concomitant metal to insulator transitions were explained within the frame work of the Zener double exchange (ZDE) model [9]. Among various mixed-valence manganites studied so far, PSMO system is of great interest for the study of the competition between the charge-ordered (CO) and charge-delocalized (CD) states. There are few reports on the magneto-transport properties of PSMO samples. Wang et al. [10] studied the strain effects on the structural and magneto-transport properties of $Pr_{0.67}Sr_{0.33}MnO_3$ thin films and found that MR is enhanced by strain-induced lattice distortions. Markovich et al. [11] studied the effect of pressure on the magnetic and transport properties of $Pr_{1-x}Sr_xMnO_3$ (x=0.22, 0.24, 0.26) crystals and observed that MR is more in sample with the pressure in comparison to the sample with zero pressure. Recently, Krishna et al. [12] systematically studied the magneto-transport properties of $Pr_{0.67}A_{0.33}MnO_3$ (A=Ca, Sr, Pb & Ba) and find highest MR ~97% for PPMO sample and lowest for PSMO sample (~50%) and explain the results on the basis of size variance parameter.

In this paper, an attempt has been made to systematically study the effect of different doping concentration of Sr (x=0.2, 0.3 and 0.5) in $Pr_{1-x}Sr_xMnO_3$ compound on their structural, magnetic and magneto-transport properties.

2. Experimental details

The PSMO samples were prepared by an improved chemical coprecipitation method. The precursors $Pr(NO_3)_3.6H_2O$, $Sr(NO_3)_2$ and $Mn(NO_3)_2.2H_2O$, with appropriate Pr :Sr: Mn atomic ratio were dissolved in de-ionized water by gentle heating. Then the aqueous mixture was slowly poured into $(NH_3)_2C_2O_4.H_2O$ solution and stirred magnetically for several minutes. The gelatinous

precipitate was filter and washed for several times using de-ionized water until the pH value of the solution became neutral. Finally, the gelatinous precipitate was dried at 150 ^{0}C in air. To prepare mono-disperse PSMO particles, the powder was dispersed by ultrasonic bath in ethanol, centrifuged and washed with ethanol. The dried powder pressed into pellets and was heat treated in air at 1200 ^{0}C for 15h. For convenience, $Pr_{1-x}Sr_xMnO_3$ samples with x=0.2, 0.3 & 0.5 are designated as PS2, PS3 and PS5, respectively. The structural characterization was examined by using X-ray diffraction (Bruker AXS D-8 advance, CuK_α radiation) technique at room temperature and surface morphology was investigated by using a field emission scanning electron microscope (FEI, Quanta 200 F, Netherlands). The elemental analysis of the sintered samples was carried out using energy dispersive X-ray analyzer (EDAX' TSL, AMETEK) coupled with FE-SEM. Resistivity as a function of temperature was measured by a standard four-probe method by using Keithley instruments without or with magnetic fields (0-10 kOe). The magnetization measurements were done by using SQUID magnetometer.

3. Results and discussion

3.1 Structural analysis

The XRD pattern of $Pr_{1-x}Sr_xMnO_3$ (x=0.2, 0.3 & 0.5) samples synthesized by co-precipitation method is shown in Fig. 1. XRD results indicate that all PS2, PS3 & PS5 samples correspond to pure PSMO orthorhombic perovskite phase except a Mn_5O_8 impurity phase (111) observed in sample PS2. We have also calculated the lattice parameters from XRD data as shown in Table 1 and found that the unit cell parameters (a, b, c) & cell volume (V) decrease as we move from sample PS2 to PS5. The decrease in unit cell parameters and cell volume with increase in Sr concentration is in agreement with the results of Markovich et al. [11].

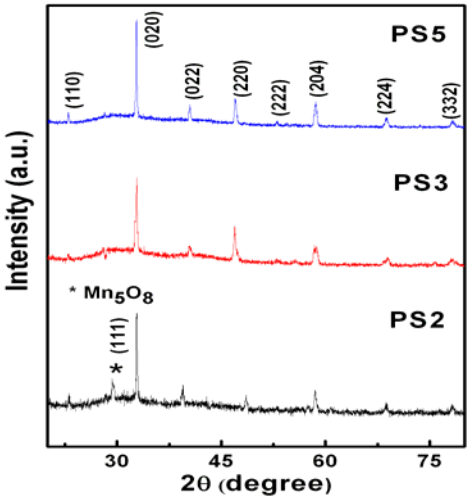

Fig. 1. XRD pattern of PS2, PS3 and PS5 samples.

Table 1. Calculated lattice parameters & unit cell volume of PS2, PS3 and PS5 samples.

Sample	a (Å)	b (Å)	c (Å)	V(Å^3)
PS2	5.485	5.479	7.784	233.92
PS3	5.474	5.476	7.740	232.01
PS5	5.432	5.445	7.734	228.75

3.2 Microstructural and chemical analysis

The representative FESEM images of the samples PS2, PS3, and PS5 are shown in Fig. 2. FESEM images reveal the good homogeneity in sample PS2 and PS5 while poor homogeneity in sample PS3. Moreover, porosity exists in all three samples. It is also found that the grain size slightly varies from ~1.1 to ~1.5 μm for the samples PS2 to PS5, respectively. The EDAX data shown in Table 2 indicates that the atomic ratio of Pr, Sr, Mn, and O is almost consistent with the nominal compositions, suggesting that the obtained PSMO samples are near to stoichiometric.

Table 2. EDAX data of PS2, PS3 and PS5 samples.

Sample	Pr (at %)	Sr (at %)	Mn (at %)	O (at %)
PS2	16.98	4.69	20.82	57.50
PS3	14.83	7.80	20.01	57.37
PS5	10.37	10.68	20.02	58.93

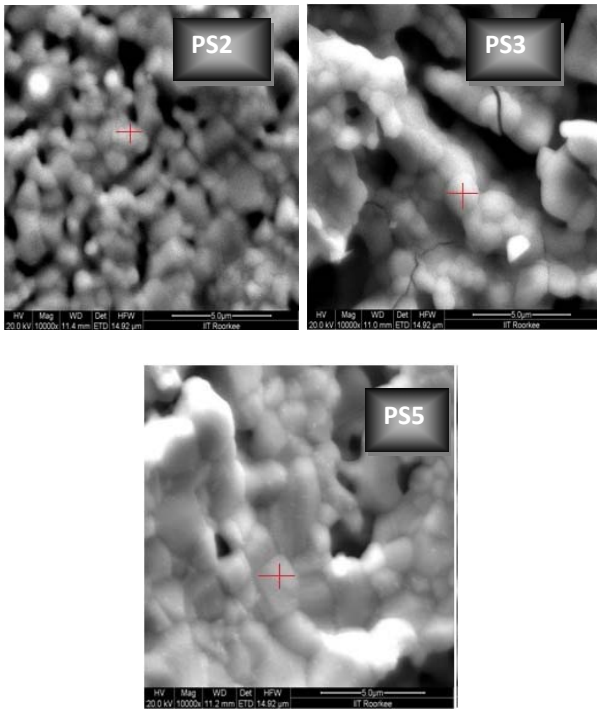

Fig. 2. FESEM micrographs of PS2, PS3 and

PS5 samples, respectively.

3.3 Magnetization studies

The magnetization versus temperature curve for all three samples in field cooled (FC) & zero field cooled (ZFC) mode measured at 500 Oe field, are shown in Fig. 3. All the samples show the paramagnetic to ferromagnetic (PM-FM) transition at a particular temperature (Tc). The transition temperatures determined from the peak in dM/dT-T curves are 103, 203 and 292 K for PS2, PS3 and PS5 sample, respectively. Along with increase in the value of Tc from 103-292 K, the value of magnetization increases for the sample PS2 and PS3 and then sharply decreases for sample PS5. Fig. 4 shows the variation of magnetization & PM-FM transition temperature with Sr doping concentration. The value of magnetization (M) at 5 K for the samples PS2, PS3, and PS5 are 11.62, 22.90 & 5.30 emu/g, respectively (as shown in Table 3). The sharp decreasing in value of magnetization of PS5 sample may be because of charge ordering phenomena in x=0.5 composition.

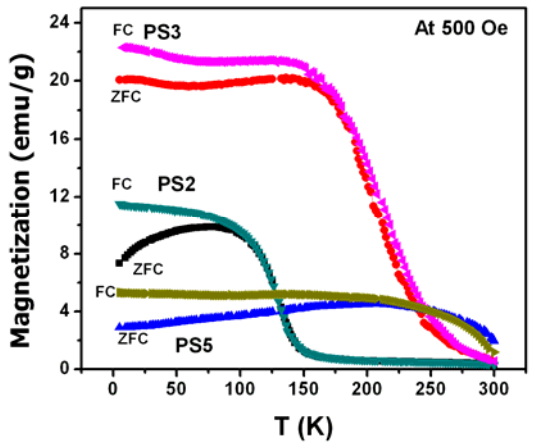

Fig. 3. Temperature dependent magnetization under ZFC & FC modes of PS2, PS3 and PS5 samples.

Furthermore, it is also observed from M-T curves that at low temperatures, M_{FC} value of all the samples are higher than those of M_{ZFC} while the M_{ZFC} & M_{FC} curves coincide above T_C. This may be attributed to the fact that at lower temperatures, the movement of magnetic domains along the magnetic field direction is restricted due to pinning of domain walls resulting in an incomplete magnetization. With increase in temperature, an increase in thermal energy allows more and more domains to align along the field direction thereby enhancing the magnetization [13]. Moreover, the gap (magnetic irreversibility) between ZFC and FC starting at the 'bifurcation point' increases with the decrease in temperature. A wide variety of systems, such as spin glasses and single domain magnetic assemblies, shows maximum magnetization in the ZFC curves. This feature can be attributed to the complex phases or to the onset of a non-equilibrium magnetic response as a result of a single domain structure and magnetic anisotropy.

Table 3. Experimental magnetic data of PS2, PS3 and PS5 samples.

Sample	T_C	M_{FC} (emu/gm) at 5K	M_{FC} (emu/gm) at H=70kOe	M_{FC} (emu/gm) at T_C
PS2	130	11.62	6.77	4.87
PS3	203	22.9	19.55	14.50
PS5	292	5.36	12.55	2.17

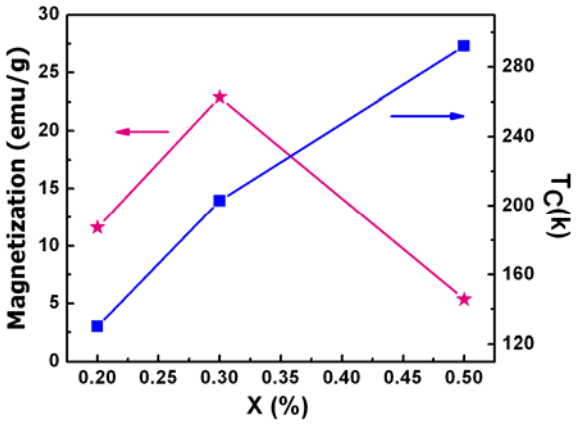

Fig. 4. Variation of Magnetization & PM-FM transition temperature with Sr content (x).

3.4 Electrical resistivity measurements

The temperature dependence of resistivity for all the samples measured at 0T, 0.5T & 1T field is shown in Fig. 5. It is observed that the value of electrical resistivity is less for PS3 (x=0.3) sample as compared to PS2 sample (x=0.2). This suggests that the doping of Sr increases the amount of Mn^{4+} ions (polaron) in $PrMnO_3$, which resulted in the improvement of $PrMnO_3$ electrical conductivity which means less the resistivity [14]. For PS5 sample, the resistivity lies between PS2 and PS3 sample. It is because for the sample x=0.5, the Mn^{4+} & Mn^{+3} ions are equal in number in per unit cell and results charge ordering in the sample. The values of resistivity are 217, 14.38, and 145 Ω-cm at 80 K for the samples PS2, PS3 and PS5, respectively. The sample PS2 and PS3 show the metal to insulator transition at temperature 102 and 143 K, respectively while sample PS5 remain semiconducting in whole measured temperature range (80-300 K). It is also

observed that the resistivity has a reduction under the applied field.

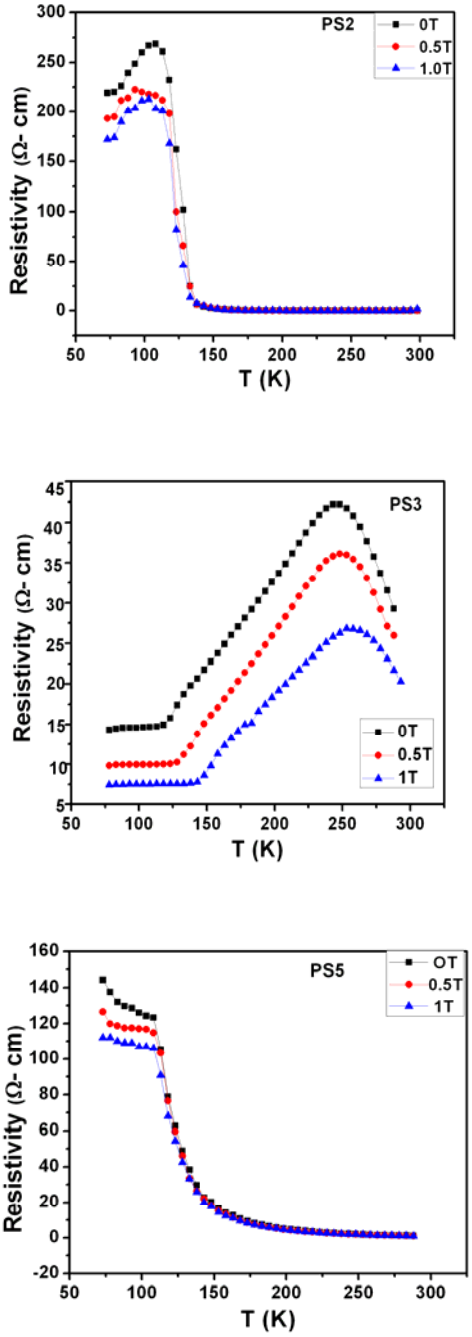

Fig. 5. Temperature dependence of resistivity at zero and an applied field H = 0.5T & 1T of PS2, PS3 & PS5 samples.

3.5 Magnetoresistance studies

The temperature dependence of Magnetoresistance (MR) for the studied samples measured in the range 80-300 K at the field of 1 T is shown in Fig. 6. The MR ratio is defined as MR (%) =[ρ(0,T) – ρ(H,T)] / ρ(H,T) × 100 %, where ρ(0,T) and ρ(H,T) are the resistivity values for zero and applied fields, respectively. In case of sample PS3 and PS5, the MR increases with decreasing the temperature. However, in case of sample PS2, MR is maximum at Curie temperature. Generally, in case of manganites, two distinct contributions of MR have been pointed out so far. One is the intrinsic MR which arises due to suppression of spin fluctuations when the spins are all aligned in the sample on application of a magnetic field. This MR has the highest value near the ferromagnetic transition temperature and decreases as the temperature decreases. This is generally observed in the case of single crystal samples and single crystal thin films [15]. On the other hand, the second type is extrinsic MR, generally observed among the polycrystalline samples and arises due to the inter-grain spin polarized tunneling across the grain boundaries and also due to domain wall contribution [16, 17]. This extrinsic kind of MR behavior is also observed in our earlier study of $La_{0.7}Sr_{0.3}MnO_3$ [18]. This extrinsic MR usually increases as the temperature decreases. Therefore, in our samples, extrinsic MR observed in PS3 and PS5 sample and intrinsic MR in sample PS2. The maximum MR at 80K is observed for the sample PS3. The MR values at 80 K, T_C & room temperature at 1T magnetic field for the samples PS2, PS3 and PS5, are shown in Table 4.

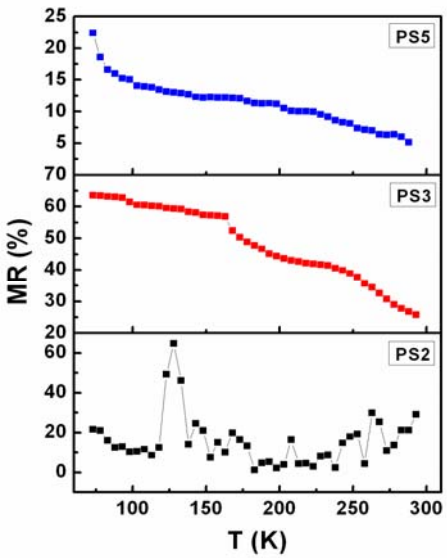

Fig. 6. Temperature dependence Magnetoresistance (MR) in a field of 1T of PS2 PS3 and PS5 samples.

Table 4. Insulator-metal transition temperature (T_{IM}), paramagnetic-ferromagnetic transition temperature (Tc), resistivity (ρ), and magnetoresistance (MR) of PS2, PS3 and PS5 samples.

Sample	T_C (K)	T_{IM} (K)	$\rho_{T=300K}$ (Ω-cm)	$\rho_{T=80K}$ (Ω-cm)	MR (%) at 1T		
					80 K	T_C (K)	300 K
PS2	130	102	1.30	217	21.74	65.33	29.58
PS3	203	243	28.90	14.38	63.41	43.25	25.0
PS5	292	110	1.8	144.56	23.09	6.68	4.9

4. Conclusions

We synthesized the $Pr_{1-x}Sr_xMnO_3$ (x = 0.2, 0.3 and 0.5) samples via improved chemical co-precipitation method and studied their structural, magnetic and magnetotransport properties. All the samples have pure PSMO phase with orthorhombic unit cells and the unit cell parameters & cell volume decrease as we move from sample x=0.2 to x=0.5. Magnetization measurements indicate all sample show the paramagnetic to ferromagnetic transition from 130 to 292 K for the sample x=0.2 to x=0.5 but value of magnetization is very weak in sample, x=0.5. Resistivity measurements show that the sample, x = 0.2 & 0.3 show the metal to insulator transition at 102 and 143 K, respectively while sample x= 0.5 remain insulating in the whole measured temperature range (80-300 K). The magnetoresistance studies show that the extrinsic MR is observed for the composition, x=0.3 and 0.5 while sample, x=0.2 shows the intrinsic type of magnetoresistance.

Acknowledgments

One of the authors Umesh Chand is grateful to the Ministry of Human Resources and Development (MHRD), New Delhi, for the award of a Fellowship.

References

[1] R. von Helmolt, J. Wecker, B. Holzapfel, L. Schultz, K. Samwer, Phys. Rev. Lett. **71**, 2331 (1993).
[2] G. A. Prinz, K. Hathaway, Phys. Today **48**(4), 24 (1995); J. L. Simonds, Phys. Today **48**(4), 26 (1995).
[3] R. Wood, IEEE Trans. Mag. **36**, 36 (2000).
[4] A. Moser, K. Takano, D. T. Margulies, M. Albrecht, Y. Sonobe Ikeda, S. Sun, E. E. Fullerton, J. Phys. D: Appl. Phys. **35**, R157 (2002).
[5] P. K. Siwach, H. K. Singh, O. N. Srivastava, J. Phys.: Condens. Matter **20**, 2732015 (2008).
[6] Y. Tokura (Ed.), Colossal Magnetoresistive Materials, Gordon and Breach Sciences Publishers, 2000.
[7] A. J. Millis, P. B. Littlewood, I. Shraiman, Phys. Rev. Lett. **74**, 5144 (1995).
[8] E. Dagotto, T. Hotta, A. Moreo, Phys. Rep. **344**, 1 (2002).
[9] C. Zener, Phys Rev B **82**, 403 (1951).
[10] H. S. Wang, E. Wertz, Y. F. Hu, Q. Li, J Appl. Phys. **87**, 7409 (2000).
[11] V. Markovich, I. Fita, R. Puzniak, A. Wisniewski, K. Suzuki, J. W. Cochrane, Y. Yuzhelevskii, Ya. M. Mukovskii, G. Gorodetsky, Phys. Rev. B **71**, 224409 (2005).
[12] D. C. Krishna, P. Venugopal Reddy, J. of Alloys & Compounds **479**, 661 (2009).
[13] J. Rivas, L. E. Hueso, A. Fondado, F. Rivadullo, M. A. Lopez-Quintela, J. Magn. Magn. Mater **221**, 57 (2000).
[14] Xiqiang Huanga, Li Peia, Zhiguo Liua, Zhe Lua, Yu Suia, Zhengnan Qiana, Wenhui Su, Journal of Alloys and Compounds **345**, 265 (2002).
[15] H. Y. Hwang, S. W. Cheong, N. P. Ong, B. Batlogg, Phys. Rev. Lett. **77**, 2041 (1996).
[16] T. Zhu, B. G. Shen, J. R. Sun, H. W. Zhao, W. S. Zhan, Appl. Phys. Lett. **78**, 3863 (2001).
[17] S. Lee, H. Y. Hwang, L. Boris, W. D. Shraiman, I. I. Ratcliff, S. W. Cheong, Phys. Rev. Lett. **82**, 4508 (1999).
[18] Anurag Gaur, G. D. Varma, J. Phys.: Condens. Matter **18**, 8837 (2006).

*Corresponding author: anuragdph@gmail.com, gdvarfph@iitr.ernet.in